Absence of *Shb* impairs insulin secretion by elevated FAK activity in pancreatic islets

Ida Alenkvist[1*], Oleg Dyachok[1*], Geng Tian[1], Jia Li[1], Saba Mehrabanfar[1], Yang Jin[2], Bryndis Birnir[2], Anders Tengholm[1] and Michael Welsh[1]

1 Department of Medical Cell Biology, Uppsala University, Uppsala, Sweden

2 Department of Neuroscience, Uppsala Universiy, Uppsala, Sweden

* indicates that these authors have contributed equally to the study

Running title: *Shb* and FAK activity in pancreatic islets

Word count: 3346

Key words: Src homology 2, FAK, insulin secretion, cAMP

Address correspondence to:

Anders Tengholm (anders.tengholm@mcb.uu.se) or

Michael Welsh (michael.welsh@mcb.uu.se)

Department of Medical Cell Biology, Uppsala University

Box 571, Husargatan 3,

75123, Uppsala, Sweden

Abstract

The Src homology-2 domain containing protein B (SHB) has previously been shown to function as a pleiotropic adapter protein conveying signals from receptor tyrosine kinases to intracellular signaling intermediates. Shb overexpression in beta-cells promotes beta-cell proliferation by increased IRS (insulin receptor substrate) and FAK (focal adhesion kinase) activity whereas *Shb* deficiency causes moderate glucose intolerance and impaired first peak insulin secretion. Using an array of techniques, including live-cell imaging, patch-clamping, immunoblotting and semi-quantitative PCR we presently investigated causes of the abnormal insulin secretory characteristics in *Shb*-knockout mice. *Shb*-knockout islets displayed an abnormal signaling signature with increased activities of FAK, insulin receptor substrate (IRS) and Akt. Beta-catenin protein expression was elevated and it showed increased nuclear localization. However, there were no major alterations of gene expression of various proteins involved in the beta-cell secretory machinery. Nor was *Shb* deficiency associated with changes in glucose-induced ATP generation or cytoplasmic Ca^{2+}-handling. In contrast, the glucose-induced rise of cAMP, known to be important for the insulin secretory response, was delayed in the *Shb*-knockout compared to wild-type control. Inhibition of FAK increased the submembrane cAMP concentration, implicating FAK activity in the regulation of insulin exocytosis. In conclusion, *Shb* deficiency causes a chronic increase of beta-cell FAK activity that perturbs the normal insulin secretory characteristics of beta-cells, suggesting multi-faceted effects of FAK on insulin secretion depending on the mechanism of FAK activation.

Introduction

Src homology-2 domain containing protein B (SHB) is a pleiotropic adapter protein generating signaling complexes in response to tyrosine kinase activation via multi-domain interactions (Anneren, et al. 2003). These complexes are context dependent and exert different roles in different settings. SHB has been found to regulate apoptosis, proliferation, differentiation and the cytoskeleton (Anneren et al. 2003). In insulin-secreting pancreatic beta-cells, SHB overexpression increases focal adhesion kinase (FAK) and insulin receptor substrate (IRS)-1/2 signaling (Welsh, et al. 2002) and proliferation (Anneren 2002) but also increases apoptosis in response to stress (Welsh, et al. 1999). FAK is a tyrosine kinase operating in submembranous focal adhesions connecting the extracellular matrix with intracellular signal transduction and the cytoskeleton (Parsons 2003). Cues from both extracellular matrix proteins and intracellular signaling events stimulate FAK activity, which in turn acts as a scaffold in focal adhesions and activates various downstream signaling pathways, such as Akt and ERK (Parsons 2003). In beta-cells, FAK has been shown to convey signals from the extracellular matrix (Hammar, et al. 2004), promoting beta cell survival, and from glucose (Arous, et al. 2013; Rondas, et al. 2011; Rondas, et al. 2012), stimulating insulin secretion both *in vitro* and *in vivo* (Cai, et al. 2012).

Absence of *Shb* has no effect on beta-cell proliferation but reduces cell death in response to cytotoxic agents (Akerblom, et al. 2009; Mokhtari, et al. 2009). In addition, Shb-deficient mice show mild glucose intolerance due to a reduction in insulin secretion (Akerblom et al. 2009). The mechanisms underlying this secretory defect are unknown. Glucose stimulation of insulin secretion involves uptake and metabolism of the sugar and the resulting production of ATP causes membrane depolarization by an inhibitory action on ATP-sensitive K^+ channels (Rorsman and

Braun 2013). The depolarization activates voltage-dependent Ca^{2+} channels and the concomitant increase of the cytoplasmic Ca^{2+} concentration ($[Ca^{2+}]_i$) triggers exocytosis of insulin secretory granules (Rorsman and Braun 2013). Glucose metabolism also stimulates the generation of cAMP and other metabolic coupling factors, which amplify the Ca^{2+}-triggered exocytosis response (Dyachok, et al. 2008; Henquin 2009). The glucose response is typically biphasic with a pronounced first phase lasting a few minutes followed by lower rate of secretion that is sustained or slowly increasing (second phase). *Shb* knockout seems to affect primarily the first phase of insulin secretion (Akerblom et al. 2009).

In the present study we investigated whether absence of *Shb* was associated with changes in ATP generation, $[Ca^{2+}]_i$, cAMP and tyrosine kinase signaling and gene expression of certain exocytotic proteins in isolated islets. There were little abnormalities in *Shb*-knockout islets. However, we observed elevated constitutive FAK activity that provides an explanation for the similarly increased activities of Akt and beta-catenin. Moreover, glucose-induced cAMP elevation was delayed, a finding that probably underlies the reduced first-peak insulin secretion, and which may occur as a consequence of increased FAK activity in *Shb*-deficient islets.

Experimental

Mice

Wild-type and *Shb*-knockout mice (Kriz, et al. 2007) on a mixed genetic background (FVBJ/C57Bl6/129Sv) of 2-5 months of age were used for islet isolation. Approval for breeding and sacrifice of mice had been given by the local animal ethics committee.

Islet isolation

Animals were killed and pancreata were removed and put into Hanks' solution (SVA, Uppsala, Sweden). Each pancreas was cut into pieces with scissors and subjected to collagenase digestion (1mg/ml Hanks/pancreas, Collagenase A, 10-154 121, Roche, Mannheim, Germany) for 20 min at 37°C, on a shaking water bath, then washed twice with wash buffer (Ringer-acetate Fresenius-Kabi, Uppsala, Sweden, supplemented with 4.5 mM $NaHCO_3$, 2.5 mM glucose and penicillin-streptomycin), and suspended in Hanks' solution. Hand-picked islets were cultured at 5.6 or 11.1 mM glucose in RPMI 1640 + 10% fetal bovine serum + antibiotics for at least 24 h before experimentation. For ATP and cAMP imaging experiments the islets were infected for 1 to 2 h with adenovirus expressing the respective protein-based signaling biosensors at a concentration of 20 plaque-forming units/cell in medium containing 2% (v/v) serum, followed by washing with regular complete medium and further culture for 16 to 20 h before use.

Immunoblotting

After 15 min incubation in Hanks' solution at 37 ^{0}C 30-50 islets were washed with ice cold PBS and directly lysed in SDS-sample buffer, boiled for 5 min and separated on SDS-PAGE. Proteins were electrophoretically transferred to Hybond-P filters (GE Healthcare). Filters were blocked in 5% BSA for one hour, after which they were probed with phospho-202/204 ERK, phospho-473 Akt, phospho-612 IRS-1/2, phospho-Y397 FAK, Akt, IRS-2, FAK, beta-catenin and ERK (Cell Signaling, Beverly, MA for most antibodies; pYFAK and pYIRS= Invitrogen, Carlsbad, CA; ERK= Santa Cruz, Santa Cruz, CA; beta-catenin= Abcam, Cambridge, UK; IRS-2=Upstate Biotechnology, Lake Placid, NY) antibodies. Bound antibodies were removed from filters by incubating for 40 min at 55°C in 2% w/v SDS and 0.1 mM β-mercaptoethanol. Horseradish peroxidase-linked goat anti-rabbit or anti-mouse were

used as secondary antibody. Immunodetection was performed as described for the ECL prime immunoblotting detection system (GE Healthcare, Uppsala, Sweden) using the Kodak Imagestation 4000MM. The intensities of the bands were quantified by densitometric scanning using Kodak Digital Science ID software (Eastman Kodak, Rochester, NY, USA).

Gene expression analysis

Total RNA was prepared by using the RNeasy mini kit (Qiagen, Hilden, Germany) with on-column DNase digestion with RNase-Free DNase set (Qiagen), according to the manufacturer's descriptions. For RNA isolation, 30 islets/sample were collected, briefly washed in PBS, then lyzed and homogenized. RNA yield was determined with a spectrophotometer at 260 nm. One-step quantitative real-time RT-PCR was performed with QuantiTect™ SYBR® Green RT-PCR-kit (Qiagen) on a LightCycler™ (Roche Diagnostics, Basel, Switzerland).

The PCR conditions were according to kit supplier's instructions: Reverse transcription 20 min 50°C, denaturation 15 min 95°C, cycling: denaturation 15 s 94°C, annealing 30 s 55-60 °C, extension 30 s 72°C. Crossing point (Ct) values were determined with the LightCycler Software v3.5. Gene expression was normalized by subtracting the corresponding β-actin Ct-value. Statistical comparisons were made on normalized Ct-values.

Measurements of cytoplasmic ATP dynamics

Islets were preincubated for 30-60 min in experimental buffer containing (in mM): NaCl 138, KCl 4.8, $MgCl_2$ 1.2, $CaCl_2$ 1.3, glucose 3, HEPES 25 (pH 7.40) and 0.5 mg/mL BSA. The islets were then placed on a poly-L-lysine-coated coverslip in the superfusion chamber on the thermostated stage of a total internal reflection fluorescence microscope (Eclipse Ti with a 60x, 1.45-NA objective, Nikon, Japan). A

diode-pumped solid state laser (Jive, Cobolt AB, Solna, Sweden) provided 488 nm excitation light and emission was selected by a 527/27 nm (centre wavelength/half-bandwidth) interference filter (Semrock, Rochester, NY, USA) and recorded by an EMCCD camera (DU-897; Andor, Belfast, UK) controlled by MetaFluor software (Molecular Devices, Sunnyvale, CA, USA). All imaging experiments were performed at 37°C, with a medium superfusion rate of 0.12 to 0.20 ml/min and with images acquired every 2-5 s.

Recordings of $[Ca^{2+}]_i$

For measurements of $[Ca^{2+}]_i$, islets were pre-incubated during 30-40 min in the presence of 1 μmol/L of the acetoxymethyl ester of the Ca^{2+} indicator Fura-PE3. Imaging of the Fura-PE3-loaded cells was performed with an inverted microscope equipped with a 40x 1.3-NA objective (Nikon) and an epifluorescence illuminator (Cairn Research Ltd, Faversham, UK) connected through a 5-mm diameter liquid light guide to an Optoscan monochromator (Cairn Research Ltd, Faversham, UK) with a 150-W xenon arc lamp. The monochromator provided excitation light at 340 and 380 nm that was reflected by a 400-nm dichroic beam splitter, and emission was measured at 510 nm/40 nm half-bandwidth using a CCD camera (Orca, Hamamatsu, Hamamatsu City, Japan) with an image intensifier (C8600, Hamamatsu). The Metafluor software (Molecular Devices) controlled the monochromator and the camera, acquiring image pairs every 2 s with 100-400 ms integration at each wavelength and <1 ms for changing wavelength and slits. To minimize bleaching and photodamage, the monochromator slits were closed until the start of the next acquisition cycle. Ratio images (340/380 nm) were obtained after subtraction of background and $[Ca^{2+}]_i$ values calculated as previously described (Grynkiewicz, et al. 1985).

Real-time measurements of cAMP

Measurements of the sub-plasma membrane concentration of cAMP were performed with a CFP/YFP-based translocation reporter and TIRF microscopy as previously described (Tian, et al. 2011). The microscope setup was the same as described for ATP measurements except that CFP and YFP excitation were provided by the 457- and 515-nm lines of diode-pumped solid-state lasers (Cobolt) and fluorescence was detected at 485/25 nm and 560/40 nm (Semrock).

Patch-clamp analysis of Ca^{2+} currents

The elecrophysiological recordings were done using whole-cell patch-clamp recordings from cells in intact islets. The extracellular solution contained in mM: 140 NaCl, 3.6 KCl, 2 $NaHCO_3$, 0.5 NaH_2PO_4, 5 Hepes (pH 7.40 with NaOH) and 2.6 $CaCl_2$. Glucose was present at 5 mM in all experiments. The pipette solution was composed of in mM: 76 K_2SO_4, 10 NaCl, 10 KCl, 1 $MgCl_2$ and 5 mM Hepes (pH 7.35 with KOH). In order to record only inward Ca2+ currents, outward currents were suppressed by the inclusion of tetraethylammonium-Cl at a concentration of 20 mM in the extracellular medium (NaCl was correspondingly reduced to maintain isosmolarity) and by replacing K_2SO_4 in the pipette-filling solution with an equimolar amount of $CsSO_4$. The recording pipettes were made from borosilicate glass capillaries (Harvard Apparatus, Holliston, MA) and had a resistance of 3-5 Mohm when filled with the pipette solution. The holding potential was set at -60 mV and then stepped to the experimental potential for 200 ms. The current recordings were done using an Axopatch 200B amplifier, filtered at 2 kHz, sampled at 10 Hz by an analog-to-digital converter and stored in a computer. The recordings were then analyzed with the pClamp 9 software (Molecular Devices).

Statistics

Means ± SEM for the indicated number of observations are given. For testing differences, Students' t-test was used (unpaired or paired depending on the experimental conditions) as indicated.

Results

Characteristics of tyrosine kinase signal transduction in *Shb*-knockout islets

Since Shb is a signal transduction protein downstream of tyrosine kinase receptors and since altered signaling characteristics were previously observed in *Shb*-deficient cells, we decided to investigate FAK, IRS1/2, Akt and ERK signaling in *Shb*-knockout islets by usage of phospho-specific antibodies recognizing active forms of these signaling intermediates (Fig 1). Basal FAK activity at 5.6 mM glucose was elevated as a consequence of absence of Shb. The increase was modest (42%) but typical for the level of increase previously observed as a consequence of *Shb* deficiency (Funa, et al. 2009; Gustafsson, et al. 2013). Downstream of FAK in beta-cells are IRS-proteins (Baron, et al. 1998). We assessed IRS-1/2 activity with an antibody that recognizes the phosphotyrosine characteristic of the active form of both proteins (pY612). Based on the total IRS-2 protein reactivity on the blots, the predominant phospho-reactive component in the current setting appeared to be IRS-2 (Fig 1). IRS-2 activity was increased by 19%. Akt and ERK are downstream of both FAK and IRS-2. Akt activity was increased by 51% whereas ERK activity showed a large variability with an average increase of 36% that failed to reach statistical significance.

One target of Akt is glycogen synthase kinase 3-beta (GSK-3b), which becomes inhibited through Akt phosphorylation (Woodgett 2005). GSK-3b is a negative

regulator of beta-catenin and consequently beta-catenin levels increase and beta-catenin translocates to the nucleus where it alters gene transcription upon Akt activation (Woodgett 2005). As Akt activity was increased in *Shb*-knockout islets, we found it relevant to investigate beta-catenin levels and nuclear translocation (Fig 2). These were both increased in *Shb*-deficient islets, suggesting that the increase in FAK activity has implications for beta-catenin dependent gene transcription via enhanced Akt activity.

Gene expression of proteins involved in exocytosis

We next determined gene expression levels of various proteins relevant to the exocytotic process using real-time RT-PCR. The genes analyzed were *Rab3a*, *Snap25* (synaptosomal-associated protein 25), *Vamp2* (vesicle-associated membrane protein 2), *Munc18-1* (*Stxbp1*, syntaxin binding protein 1) and *Stx1a* (Syntaxin1a) (Table 1). None of these was differentially expressed in *Shb*-knockout islets compared with control islets, suggesting that altered expression of these exocytosis proteins are not likely explanations for the reduced first-phase insulin secretory response.

Sub-membrane ATP levels and intracellular Ca^{2+} handling in *Shb*-knockout islets

To investigate whether abnormalities in glucose stimulus-secretion coupling can explain the secretory defect we measured the submembrane ATP concentration with TIRF microscopy and the fluorescent ATP sensor Perceval in islets exposed to a step increase in glucose concentration from 3 to 20 mM. This stimulation resulted in a pronounced rise of ATP (Fig 3), which was of similar magnitude in both wild-type (48±3% increase of Perceval fluorescence) and *Shb*-knockout (50±2%) islets ($p>0.6$) suggesting that absence of Shb does not impair the ability of beta cells to generate ATP in response to glucose stimulation.

The rise of sub-membrane ATP triggers depolarization and voltage-dependent Ca^{2+} influx in beta-cells. The resulting increase of $[Ca^{2+}]_i$ was investigated as a potential explanation for the aberrant insulin secretory characteristics. Slight tendencies to lower $[Ca^{2+}]_i$ in *Shb*-knockout islets in the presence of both 3 and 20 mM glucose did not reach statistical signficance (Fig 4). Moreover, closure of ATP-sensitive K^+ channels with 1 mM tolbutamide resulted in similar increases of $[Ca^{2+}]_i$. Patch-clamp analysis of whole-cell Ca^{2+} currents in beta-cells from intact islets also failed to demonstrate any difference between wild-type and *Shb*-knockout cells (Fig 5), suggesting that the defective insulin secretion is not due to alterations of intracellular Ca^{2+} handling.

Glucose-induced cAMP generation is delayed in *Shb*-knockout islets

First peak insulin secretion has been found to relate to cAMP generation (Idevall-Hagren, et al. 2010) and we therefore investigated the dynamics of glucose-induced cAMP generation. Interestingly, the rise of cAMP triggered by an elevation of the glucose concentration from 3 to 20 mM was delayed by approximately one minute in *Shb*-knockout islets compared to control (Fig 6). This provides a potential explanation for the impaired first-peak insulin secretory response observed in these islets.

Inhibition of FAK triggers rise of sub-membrane cAMP

Increased FAK activity has previously been reported to stimulate insulin secretion in response to glucose stimulation (Rondas et al. 2011). We decided to address whether FAK activity can be related to insulin secretion also in the current setting by monitoring the submembrane cAMP concentration since active FAK has been shown to recruit a cAMP-degrading phosphodiesterase (Serrels, et al. 2011; Serrels, et al. 2010). Addition of 10 μM of the FAK inhibitor 14 (Golubovskaya, et al. 2008; Gustafsson et al. 2013) to MIN6 cells, wild-type islets and *Shb*-knockout islets

exposed to 3 mM glucose caused a progressive increase in the basal cAMP concentration (Fig 7), suggesting that FAK indeed may exert negative control of cAMP signaling.

Discussion

Shb was originally described as a serum-inducible gene in beta-cells (Welsh, et al. 1994) but subsequently found to be a ubiquitously expressed adapter protein with pleiotropic functions (Anneren et al. 2003). The multi-domain structure of Shb allows the generation of signaling complexes and these can propagate signals of great diversity. A recent study describes binding of four key beta-cell transcription factors (PDX1, NKX2.2, FOXA2 and NKX6.1) to a cluster of binding sites in the *SHB* gene (Pasquali, et al. 2014), suggesting the importance of Shb in relation to beta-cell function and possibly also for the development of type 2 diabetes.

Shb has been found to interact with FAK (Holmqvist, et al. 2003). It is thought that Shb bridges an active tyrosine kinase receptor and FAK while simultaneously binding c-Src, thus promoting FAK activation within this multi-component complex (Anneren et al. 2003; Holmqvist et al. 2003). In insulin producing cells, Shb overexpression increases the association between FAK and IRS-1, thus augmenting IRS signaling (Welsh et al. 2002). Surprisingly, *Shb* deficient cells commonly display elevated basal FAK activity (Funa et al. 2009; Gustafsson et al. 2013; Zang, et al. 2013) with reduced ligand-responsiveness but the reason behind this response has not been clarified. One possible interpretation of those findings is that the elevated basal FAK activity is an adaptive response to loss of the ability of ligands to induce FAK activation although it is also possible that Shb associates with or regulates the activity of other signaling components that down-regulate FAK activity. The presently

described moderate increase in basal FAK activity is in line with studies on endothelial and hematopoietic cells demonstrating a similar effect of *Shb* deficiency (Funa et al. 2009; Gustafsson et al. 2013).

The increase in IRS-2 and Akt activities are likely consequences of elevated FAK phosphorylation (Cai et al. 2012). Absence of *Shb* renders beta-cells less prone to apoptosis upon cytokine exposure and this is likely due to the activation of Akt (Bernal-Mizrachi, et al. 2001; Elghazi, et al. 2007). One consequence of Akt activation is phosphorylation of the beta-catenin regulator GSK-3b, leading to increased expression of beta-catenin and its nuclear translocation (Elghazi et al. 2007). This will participate in the anti-apoptotic effect of Akt via changes in gene transcription (Elghazi et al. 2007).

Even if the expression of many genes can be expected to be altered as a consequence of *Shb*-gene knockout and the associated increase in FAK and Akt activities, we did not find changes in the expression of genes directly involved in the exocytosis machinery, suggesting that alterations in insulin secretion had other causes. Investigation of stimulus-secretion coupling by live-cell imaging of various signaling events showed that glucose-induced ATP formation and voltage-dependent Ca^{2+} influx was normal in *Shb*-knockout beta-cells. Instead, the most striking finding in these cells was delayed glucose-induced cAMP production. Since cAMP is crucial not only in amplification of insulin secretion by incretin hormones, but also for the normal glucose-induced insulin secretory response (Dyachok et al. 2008), we suggest that this defect may explain the reduced first phase insulin secretion in the absence of *Shb*. The mechanism underlying the altered cAMP signaling is unknown. However, it is interesting to note that a consequence of elevated FAK activity is the recruitment of phosphodiesterase 4D5 to focal adhesions, invoking a decreased cAMP concentration

in the submembrane compartment adjacent to focal adhesions (Serrels et al. 2011; Serrels et al. 2010). A similar mechanism whereby FAK regulates the submembrane cAMP concentration may be present also in beta-cells and FAK-inhibition was accordingly found to cause an increase of the basal cAMP concentration, possibly by release of phosphodiesterases from the dissolving focal adhesions.

FAK has been shown to exert positive cues in glucose-stimulated insulin secretion (Arous et al. 2013; Cai et al. 2012; Rondas et al. 2011; Rondas et al. 2012) but the present data indicate that FAK may serve an inhibitory role in this process as well. FAK inhibition reduced both first- and second-phase glucose-stimulated insulin secretion and reduced the number of docked granules (Rondas et al. 2011; Rondas et al. 2012) indicating that the prevailing effect of FAK is to promote the exocytotic process. *Shb* knockout islets exhibiting elevated basal FAK activity, on the other hand, display elevated basal insulin secretion, reduced first-phase secretion and reduced numbers of docked granules (Akerblom et al. 2009), suggesting that the dual effect of FAK becomes most apparent when related to the significant reduction of first-phase secretion noted in the *Shb* knockout system. This would imply that chronic FAK-stimulation exerts compensatory changes that are detrimental to the first-phase secretory process whereas stimulatory effects of FAK prevail under the other situations. The most apparent consequence of the altered FAK response in the *Shb* knockout islets is the delayed cAMP response to glucose-stimulation, providing a plausible explanation for the reduced first-phase response.

In summary, absence of *Shb* causes a chronic activation of FAK by an unknown mechanism. This will change certain signaling characteristics, such as activation of IRS-2, Akt and beta-catenin. The beta-cell undergoes adaptive responses with reduced

cell toxicity and first-phase glucose-induced insulin secretion. The latter seems to be a consequence of FAK-mediated suppression of submembrane cAMP signaling.

Conflicts of interest

The authors declare no conflicts of interest

Author contribution

AT and MW designed the experiments, IA, OD, GT, JL, SM, YJ and MW performed the experiments, IA, OD, GT YJ, BB, AT and MW analyzed the data and AT and MW wrote the paper.

Funding

The study was supported by grants from the Swedish Diabetes Fund, the Swedish Cancer Fund, the family Ernfors Fund, the Novo-Nordisk Foundation, EFSD/MSD and the Swedish research Council.

Acknowledgements

We are grateful to Dr Sebastian Barg for suggestions and discussion.

References

Akerblom B, Barg S, Calounova G, Mokhtari D, Jansson L & Welsh M 2009 Impaired glucose homeostasis in Shb-/- mice. *J Endocrinol* **203** 271-279.

Anneren C 2002 Dual role of the tyrosine kinase GTK and the adaptor protein SHB in beta-cell growth: enhanced beta-cell replication after 60% pancreatectomy and increased sensitivity to streptozotocin. *The Journal of endocrinology* **172** 145-153.

Anneren C, Lindholm CK, Kriz V & Welsh M 2003 The FRK/RAK-SHB signaling cascade: a versatile signal-transduction pathway that regulates cell survival, differentiation and proliferation. *Curr Mol Med* **3** 313-324.

Arous C, Rondas D & Halban PA 2013 Non-muscle myosin IIA is involved in focal adhesion and actin remodelling controlling glucose-stimulated insulin secretion. *Diabetologia* **56** 792-802.

Baron V, Calleja V, Ferrari P, Alengrin F & Van Obberghen E 1998 p125Fak focal adhesion kinase is a substrate for the insulin and insulin-like growth factor-I tyrosine kinase receptors. *The Journal of biological chemistry* **273** 7162-7168.

Bernal-Mizrachi E, Wen W, Stahlhut S, Welling CM & Permutt MA 2001 Islet beta cell expression of constitutively active Akt1/PKB alpha induces striking hypertrophy, hyperplasia, and hyperinsulinemia. *The Journal of clinical investigation* **108** 1631-1638.

Cai EP, Casimir M, Schroer SA, Luk CT, Shi SY, Choi D, Dai XQ, Hajmrle C, Spigelman AF, Zhu D, et al. 2012 In vivo role of focal adhesion kinase in regulating pancreatic beta-cell mass and function through insulin signaling, actin dynamics, and granule trafficking. *Diabetes* **61** 1708-1718.

Dyachok O, Idevall-Hagren O, Sagetorp J, Tian G, Wuttke A, Arrieumerlou C, Akusjarvi G, Gylfe E & Tengholm A 2008 Glucose-induced cyclic AMP oscillations regulate pulsatile insulin secretion. *Cell metabolism* **8** 26-37.

Elghazi L, Rachdi L, Weiss AJ, Cras-Meneur C & Bernal-Mizrachi E 2007 Regulation of beta-cell mass and function by the Akt/protein kinase B signalling pathway. *Diabetes, obesity & metabolism* **9 Suppl 2** 147-157.

Funa NS, Kriz V, Zang G, Calounova G, Akerblom B, Mares J, Larsson E, Sun Y, Betsholtz C & Welsh M 2009 Dysfunctional microvasculature as a consequence of shb gene inactivation causes impaired tumor growth. *Cancer Res* **69** 2141-2148.

Golubovskaya VM, Nyberg C, Zheng M, Kweh F, Magis A, Ostrov D & Cance WG 2008 A small molecule inhibitor, 1,2,4,5-benzenetetraamine tetrahydrochloride, targeting the y397 site of focal adhesion kinase decreases tumor growth. *Journal of medicinal chemistry* **51** 7405-7416.

Grynkiewicz G, Poenie M & Tsien RY 1985 A new generation of Ca2+ indicators with greatly improved fluorescence properties. *The Journal of biological chemistry* **260** 3440-3450.

Gustafsson K, Heffner G, Wenzel PL, Curran M, Grawe J, McKinney-Freeman SL, Daley GQ & Welsh M 2013 The Src homology 2 protein Shb promotes cell cycle progression in murine hematopoietic stem cells by regulation of focal adhesion kinase activity. *Experimental cell research* **319** 1852-1864.

Hammar E, Parnaud G, Bosco D, Perriraz N, Maedler K, Donath M, Rouiller DG & Halban PA 2004 Extracellular matrix protects pancreatic beta-cells against apoptosis: role of short- and long-term signaling pathways. *Diabetes* **53** 2034-2041.

Henquin JC 2009 Regulation of insulin secretion: a matter of phase control and amplitude modulation. *Diabetologia* **52** 739-751.

Holmqvist K, Cross M, Riley D & Welsh M 2003 The Shb adaptor protein causes Src-dependent cell spreading and activation of focal adhesion kinase in murine brain endothelial cells. *Cell Signal* **15** 171-179.

Idevall-Hagren O, Barg S, Gylfe E & Tengholm A 2010 cAMP mediators of pulsatile insulin secretion from glucose-stimulated single beta-cells. *The Journal of biological chemistry* **285** 23007-23018.

Kriz V, Mares J, Wentzel P, Funa NS, Calounova G, Zhang XQ, Forsberg-Nilsson K, Forsberg M & Welsh M 2007 Shb null allele is inherited with a transmission ratio distortion and causes reduced viability in utero. *Dev Dyn* **236** 2485-2492.

Mokhtari D, Kerblom B, Mehmeti I, Wang X, Funa NS, Olerud J, Lenzen S, Welsh N & Welsh M 2009 Increased Hsp70 expression attenuates cytokine-induced cell death in islets of Langerhans from Shb knockout mice. *Biochem Biophys Res Commun*.

Parsons JT 2003 Focal adhesion kinase: the first ten years. *J Cell Sci* **116** 1409-1416.

Pasquali L, Gaulton KJ, Rodriguez-Segui SA, Mularoni L, Miguel-Escalada I, Akerman I, Tena JJ, Moran I, Gomez-Marin C, van de Bunt M, et al. 2014 Pancreatic islet enhancer clusters enriched in type 2 diabetes risk-associated variants. *Nature genetics* **46** 136-143.

Rondas D, Tomas A & Halban PA 2011 Focal adhesion remodeling is crucial for glucose-stimulated insulin secretion and involves activation of focal adhesion kinase and paxillin. *Diabetes* **60** 1146-1157.

Rondas D, Tomas A, Soto-Ribeiro M, Wehrle-Haller B & Halban PA 2012 Novel mechanistic link between focal adhesion remodeling and glucose-stimulated insulin secretion. *The Journal of biological chemistry* **287** 2423-2436.

Rorsman P & Braun M 2013 Regulation of insulin secretion in human pancreatic islets. *Annual review of physiology* **75** 155-179.

Serrels B, Sandilands E & Frame MC 2011 Signaling of the direction-sensing FAK/RACK1/PDE4D5 complex to the small GTPase Rap1. *Small GTPases* **2** 54-61.

Serrels B, Sandilands E, Serrels A, Baillie G, Houslay MD, Brunton VG, Canel M, Machesky LM, Anderson KI & Frame MC 2010 A complex between FAK, RACK1, and PDE4D5 controls spreading initiation and cancer cell polarity. *Current biology : CB* **20** 1086-1092.

Tian G, Sandler S, Gylfe E & Tengholm A 2011 Glucose- and hormone-induced cAMP oscillations in alpha- and beta-cells within intact pancreatic islets. *Diabetes* **60** 1535-1543.

Welsh M, Christmansson L, Karlsson T, Sandler S & Welsh N 1999 Transgenic mice expressing Shb adaptor protein under the control of rat insulin promoter exhibit altered viability of pancreatic islet cells. *Mol Med* **5** 169-180.

Welsh M, Mares J, Karlsson T, Lavergne C, Breant B & Claesson-Welsh L 1994 Shb is a ubiquitously expressed Src homology 2 protein. *Oncogene* **9** 19-27.

Welsh N, Makeeva N & Welsh M 2002 Overexpression of the Shb SH2 domain-protein in insulin-producing cells leads to altered signaling through the IRS-1 and IRS-2 proteins. *Mol Med* **8** 695-704.

Woodgett JR 2005 Recent advances in the protein kinase B signaling pathway. *Current opinion in cell biology* **17** 150-157.

Zang G, Christoffersson G, Tian G, Harun-Or-Rashid M, Vagesjo E, Phillipson M, Barg S, Tengholm A & Welsh M 2013 Aberrant association between vascular endothelial growth factor receptor-2 and VE-cadherin in response to vascular endothelial growth factor-a in Shb-deficient lung endothelial cells. *Cellular signalling* **25** 85-92.

Figure legends

Figure 1: Activities of FAK, IRS-2, Akt and ERK in wild-type and *Shb*-knockout islets as determined by western blot analysis using phospho-specific antibodies recognizing active forms. Isolated islets were cultured over-night in RPMI 1640 + 10% fetal bovine serum, incubated at 37 ^{0}C for 15 min in Hanks' salt solution containing 5.6 mM glucose prior to lysis, electrophoresis, blotting and incubation with appropriate antibodies. Relative values after densitometry are given as means ± SEM for 5-6 separate experiments (separate islet isolation and blot). In the pERK and total ERK blots, bands from the same blot with an identical exposure were juxtaposed. * indicates $p < 0.05$ with a paired Students' t-test.

Figure 2: Contents and nuclear translocation of beta catenin in wild-type and *Shb*-knockout islets. For expression, islets were analyzed as in Fig. 1. Values are relative expression after quantification for total ERK. Nuclear translocation was determined on images as shown, in which dapi-positive nuclei (blue) were also positive for beta-catenin staining (green). Relative fractions of positive nuclei were scored. Means ± SEM for 6 separate experiments are shown. * and ** indicate $p< 0.05$ and $p< 0.01$, respectively, using a paired Students t-test.

Figure 3: Glucose-induced ATP generation in wildtype and *Shb*-knockout islets. Representative TIRF microscopy recordings of the sub-membrane ATP concentration in superficially located cells in Perceval expressing wild-type and Shb-knockout islets during an increase of the glucose concentration from 3 to 20 mM.

Figure 4: $[Ca^{2+}]_i$ recordings from wild-type and *Shb*-knockout islets. Islets were sequentially exposed to 0.25 mM diazoxide, 1 mM tolbutamide and 20 mM glucose as indicated. The bar diagram shows means ± SEM for the amplitudes of the initial

glucose- and tolbutamide-triggered $[Ca^{2+}]_i$ increases from 4-8 experiments. Basal $[Ca^{2+}]_i$ was 114± 8 nM for wt and 92 ± 6 nM for ko.

Figure 5: Ca^{2+}-channel activity in wild-type and *Shb*-knockout islets. The data points show the average ± SEM whole-cell current response from wild-type (n =7, black circle) and KO (n = 10, open circle) cells. The holding potential was -60 mV and the test pulse was applied for 200 ms.

Figure 6: Delayed increase of cAMP in response to 20 mM glucose in *Shb*-knockout islets. A, TIRF microscopy recordings of the sub-membrane cAMP concentration in single cells within intact wild-type (black trace) and Shb knockout (dashed grey trace) islets during increase of the glucose concentration from 3 to 20 mM. B, Quantification of the delay between glucose stimulation and rise of cAMP in wild-type and Shb-knockout islet cells. Means ± SEM for 6 separate experiments are shown. * indicates $p<0.05$ with an unpaired Students' t-test. C, Effect of 10 μM of FAK inhibitor 14 on cAMP in a wildtype islet exposed to 3 mM glucose. D, Corresponding results from a *Shb*-knockout islet.

Table 1: Expression of genes coding for exocytotic proteins in *Shb*-knockout islets.

Gene	Wild-type	*Shb*-knockout
Rab3a	5.04± 0.42	5.15± 0.39
Snap25	3.79± 0.47	4.09± 0.31
Munc18-1 (Stxbp1)	3.99± 0.25	4.34± 0.32
Vamp2	2.86± 0.61	2.99± 0.56
Syntaxin1a (Stx1a)	10.42± 0.96	10.25± 0.97

Values are Ct values after subtracting the corresponding beta actin Ct values. Means± SEM are shown for 6-11 separate experiments.

Figure 1

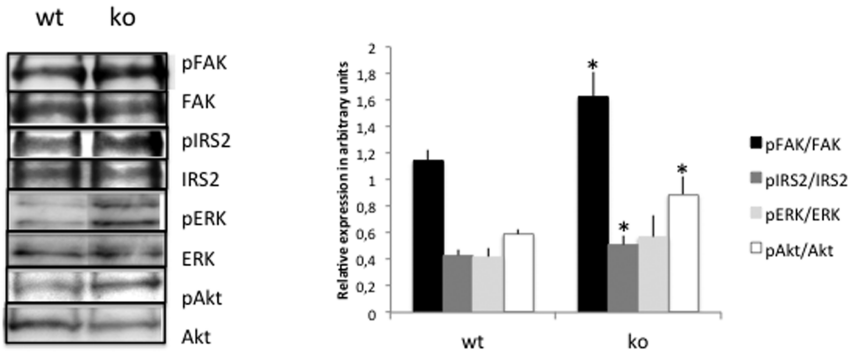
wt
ko
pFAK
FAK
pIRS2
IRS2
pERK
ERK
pAkt
Akt
Relative expression in arbitrary units
2
1,8
1,6
1,4
1,2
1
0,8
0,6
0,4
0,2
0
*
*
*
wt
ko
pFAK/FAK
pIRS2/IRS2
pERK/ERK
pAkt/Akt

Figure 2

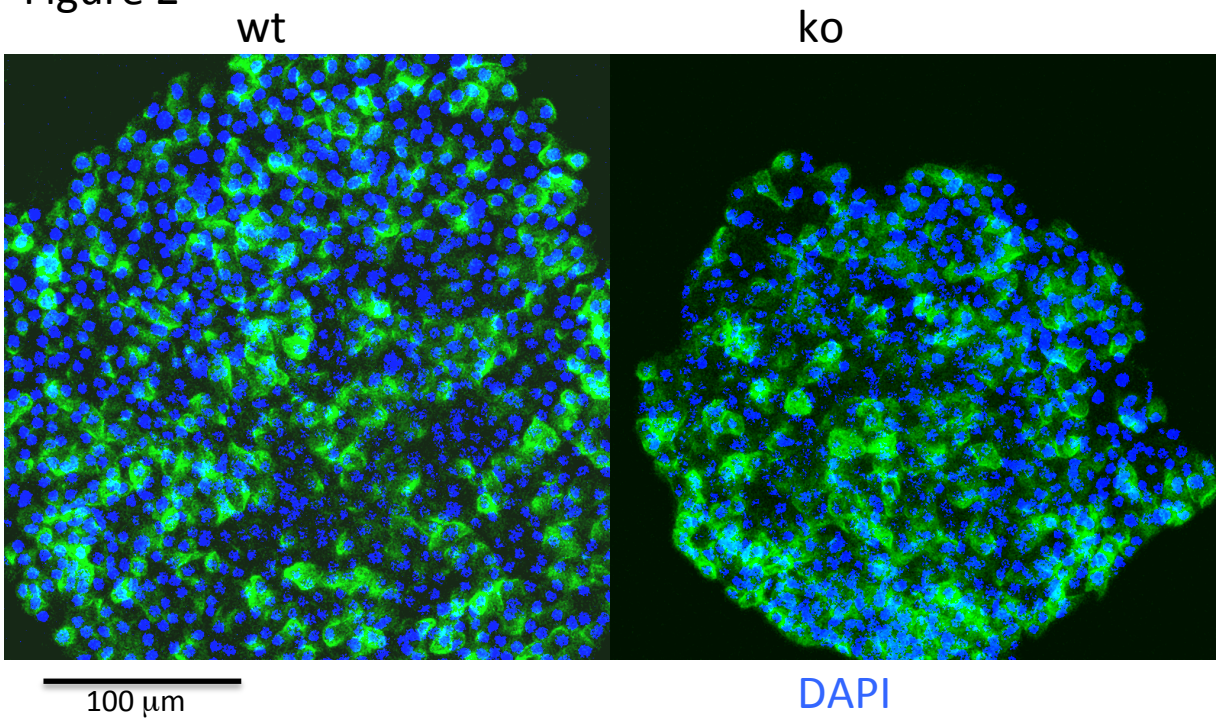
wt
ko
100 μm
DAPI
beta-catenin

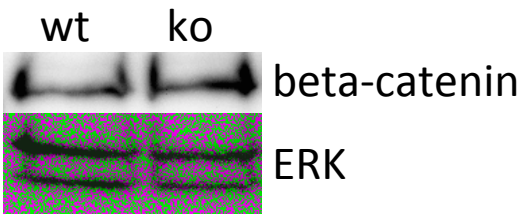
wt
ko
beta-catenin
ERK

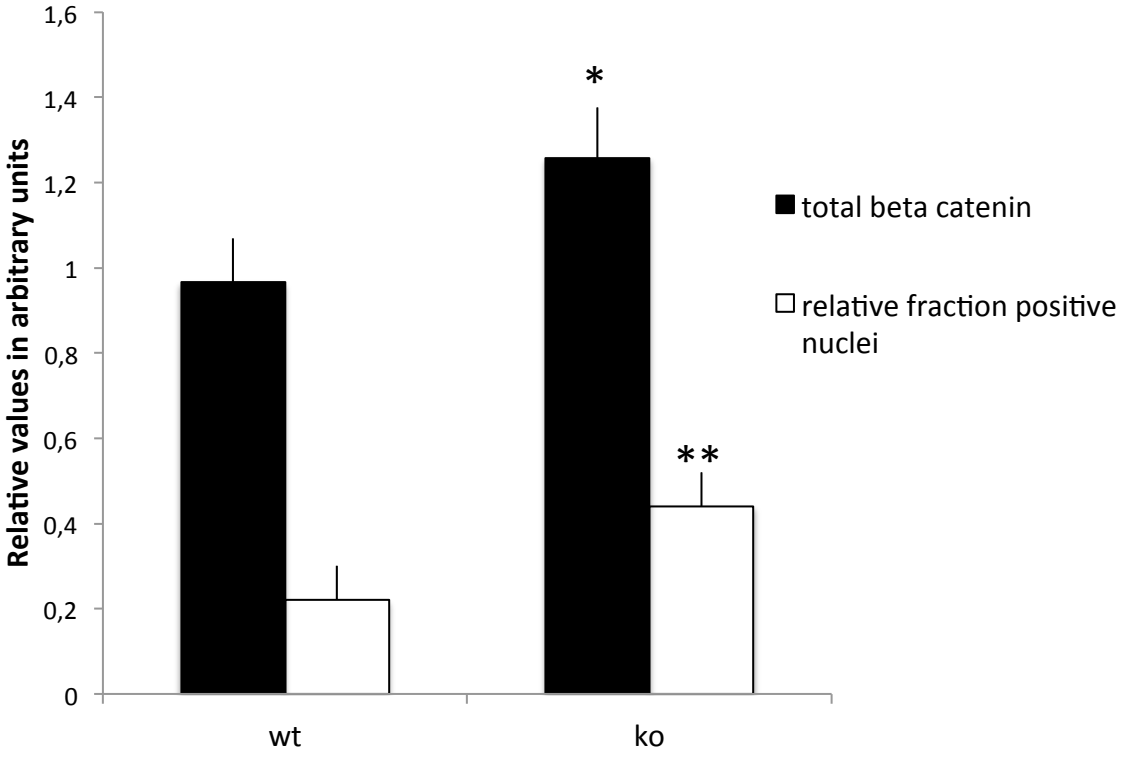
Relative values in arbitrary units
1,6
1,4
1,2
1
0,8
0,6
0,4
0,2
0
*
**
wt
ko
total beta catenin
relative fraction positive nuclei

Figure 3

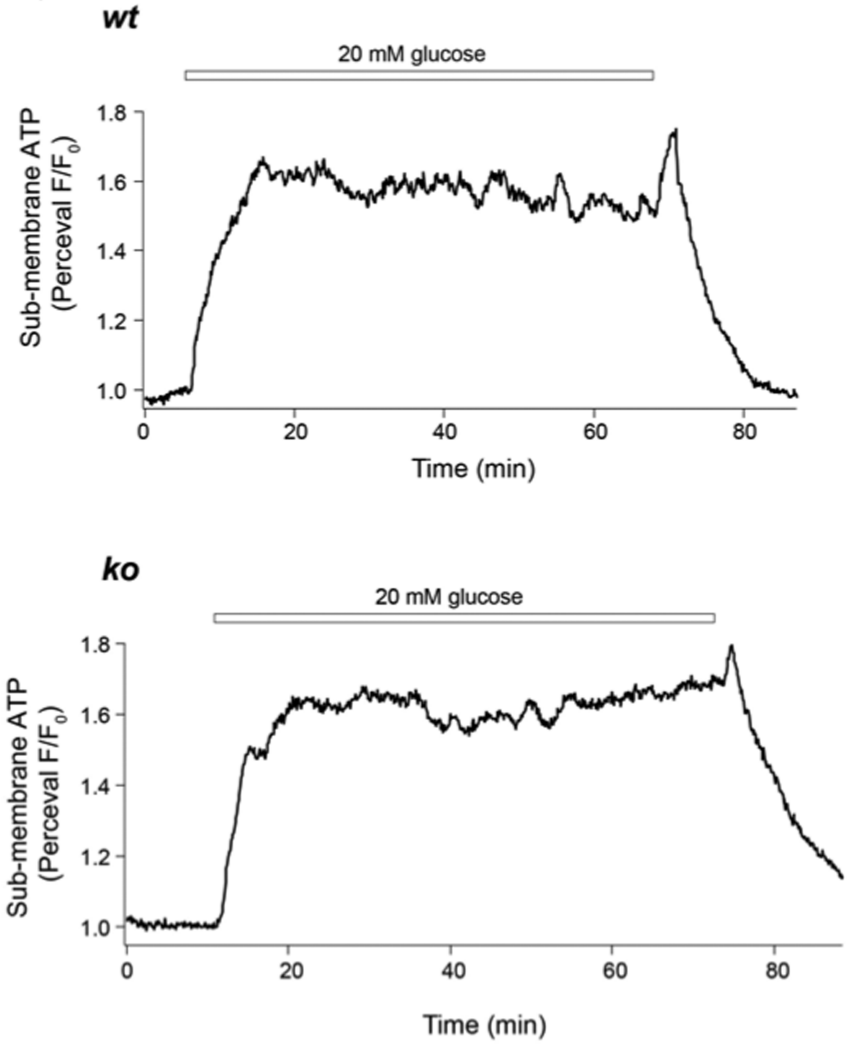
wt
20 mM glucose
Sub-membrane ATP
(Perceval F/F0)
1.8
1.6
1.4
1.2
1.0
0
20
40
60
80
Time (min)
ko
20 mM glucose
Sub-membrane ATP
(Perceval F/F0)
1.8
1.6
1.4
1.2
1.0
0
20
40
60
80
Time (min)

Figure 4

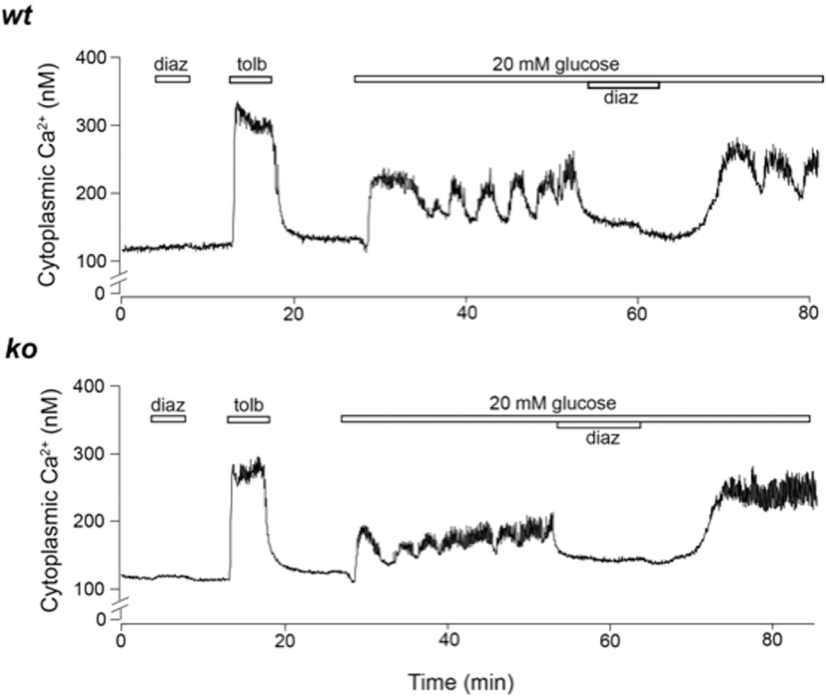
wt
diaz
tolb
20 mM glucose
diaz
Cytoplasmic Ca2+ (nM)
400
300
200
100
0
0
20
40
60
80
ko
diaz
tolb
20 mM glucose
diaz
Cytoplasmic Ca2+ (nM)
400
300
200
100
0
0
20
40
60
80
Time (min)

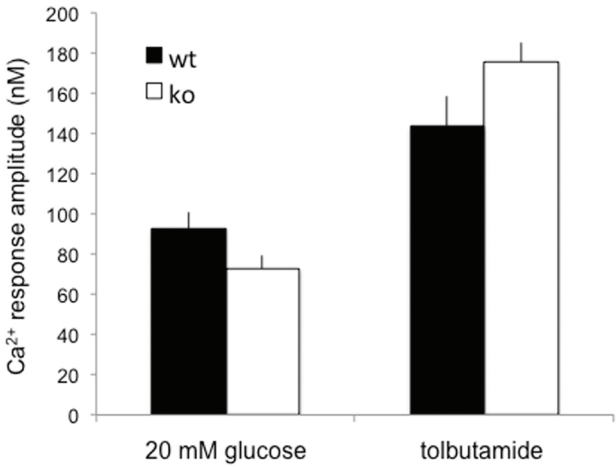
wt
ko
Ca2+ response amplitude (nM)
200
180
160
140
120
100
80
60
40
20
0
20 mM glucose
tolbutamide

Figure 5

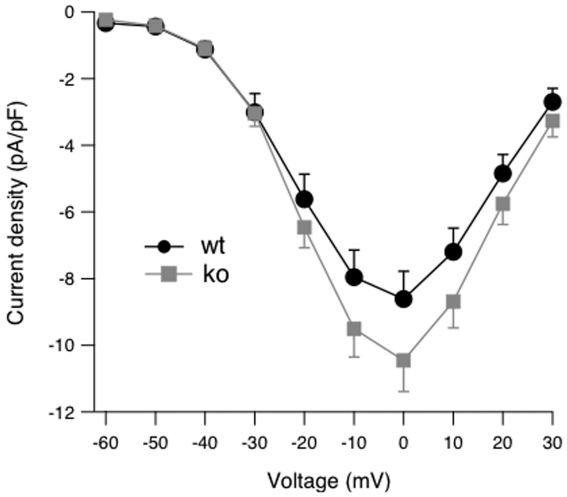
Current density (pA/pF)
0
-2
-4
-6
-8
-10
-12
wt
ko
-60
-50
-40
-30
-20
-10
0
10
20
30
Voltage (mV)

Figure 6

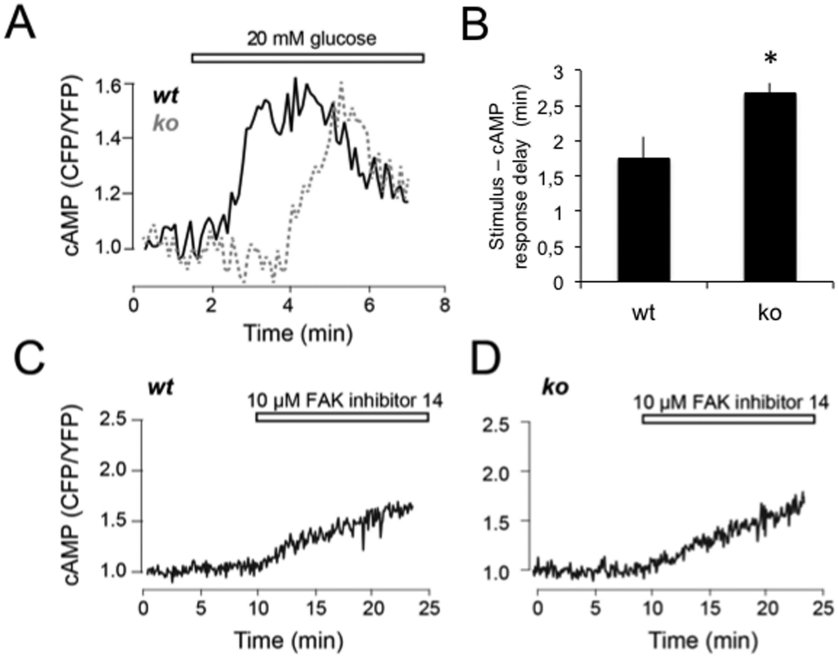
A
20 mM glucose
wt
ko
cAMP (CFP/YFP)
1.6
1.4
1.2
1.0
0
2
4
6
8
Time (min)
B
*
Stimulus – cAMP response delay (min)
3
2,5
2
1,5
1
0,5
0
wt
ko
C
wt
10 µM FAK inhibitor 14
cAMP (CFP/YFP)
2.5
2.0
1.5
1.0
0
5
10
15
20
25
Time (min)
D
ko
10 µM FAK inhibitor 14
2.5
2.0
1.5
1.0
0
5
10
15
20
25
Time (min)